

Primljen / Received: 11.5.2019.

Ispravljen / Corrected: 17.3.2021.

Prihvaćen / Accepted: 16.5.2022.

Dostupno online / Available online: 10.7.2022.

# Determination of permanent deformation of flexible pavements using finite element model

## Authors:



Hüseyin Karadağ, PhD. CE

Ministry of Family, Labour and Social Services,  
Turkey

[karatagh@hotmail.com](mailto:karatagh@hotmail.com)

Corresponding author

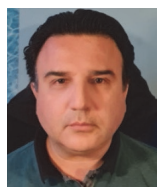


Prof. Seyhan Firat, PhD. CE

Gazi University, Turkey

Department of Civil Engineering

[sfirat@gazi.edu.tr](mailto:sfirat@gazi.edu.tr)



Prof. Nihat Sinan Isik, PhD. CE

Gazi University, Turkey

Department of Civil Engineering

[nihatsinan@gazi.edu.tr](mailto:nihatsinan@gazi.edu.tr)



Prof. Gülgün Yılmaz, PhD. CE

Eskisehir Technical University, Turkey

Department of Civil Engineering

[gulgunyilmaz@eskisehir.edu.tr](mailto:gulgunyilmaz@eskisehir.edu.tr)

Research Paper

[Huseyin Karadag](#), [Seyhan Firat](#), [Nihat Sinan Isik](#), [Gulgun Yilmaz](#)

## Determination of permanent deformation of flexible pavements using finite element model

The unbound granular material used in flexible road pavements exhibits an elastoplastic behaviour under repetitive traffic loads. Permanent deformation occurring on pavement surface under traffic load is one of the main road pavement problems affecting road performance. Therefore, many permanent deformation models for calculating road pavement rutting have recently been developed by researchers. Most of these studies involve performance of dynamic triaxial tests. In this study, deformation characteristics of unbound granular materials are determined using the resonant column test. Then, instead of determining the total permanent deformation by summing up the calculated permanent deformations obtained in each pavement layer, dynamic 2D axisymmetric finite element analyses are performed for four different pavement cross sections to predict the total permanent deformation occurring on pavement surface under certain load cycles. The first modelled cross section of unbound granular material consists of natural aggregate. The base and/or subbase of remaining three cross sections consists of steel slag waste material. The permanent deformation versus load cycle is presented for four multi-layer road cross sections using semi logarithmic graphs. Finally, the permanent deformation model equation is developed for each pavement cross section using their fitting curves.

### Key words:

pavement, finite element method, dynamic analysis, road base, steel slag

Prethodno priopćenje

[Huseyin Karadag](#), [Seyhan Firat](#), [Nihat Sinan Isik](#), [Gulgun Yilmaz](#)

## Određivanje trajnih deformacija savitljivih kolničkih konstrukcija pomoću metode konačnih elemenata

Nevezani zrnati materijal koji se koristi u savitljivim kolničkim konstrukcijama ponaša se elastoplastično pod utjecajem ponavljanih prometnih opterećenja. Trajne deformacije koje se javljaju na površini kolnika uslijed prometnog opterećenja jedan su od osnovnih problema koji negativno utječu na ponašanje kolničkih konstrukcija. Zbog toga su u novije vrijeme razvijeni brojni modeli za analizu trajnih deformacija, tj. za izračunavanje pojave kolotruga na kolnicima. Većina istraživanja koja se bave tim pitanjem temelje se na provedbi dinamičkih troosnih ispitivanja. U ovom je istraživanju deformabilnost nevezanih zrnatih materijala određena ispitivanjem prema metodi rezonantnog stupca. Također, umjesto određivanja ukupnih trajnih deformacija zbrajanjem izračunanih deformacija pojedinačnih slojeva kolnika, u ovom se radu na četiri različita tipa kolničkih konstrukcija provode dinamičke dvodimenzionalne osnosimetrične analize metodom konačnih elemenata kako bi se predvidjela ukupna trajna deformacija koja se javlja na površini kolnika nakon određenog broja ciklusa opterećenja. Nevezani slojevi za prvi modelirani tip kolničke konstrukcije sastoje se od prirodnog agregata. Nevezani nosivi sloj i/ili tamponski sloj preostalih triju kolničkih konstrukcija sastoji se od otpadnog materijala čelične zgure. Odnos trajnih deformacija i broja ciklusa opterećenja za sva četiri tipa kolničkih konstrukcija prikazan je na polulogaritamskim dijagramima. Za svaki je analizirani tip kolničke konstrukcije prikazana jednadžba trajnih deformacija.

### Ključne riječi:

kolnička konstrukcija, metoda konačnih elemenata, dinamička analiza, nosivi sloj, čelična zgura

## 1. Introduction

As road structures are quite complex, they are modelled by analytical, numerical, and experimental techniques. This complex behaviour should be well understood and so any road structure, such as pavement and subgrade, requires elaborate predictive methods aimed at assessing the long-term performance of each particular type of geotechnical structures. One of major concerns is the ability to determine dynamic stresses and deformations of road structures induced by repeated traffic load [1].

The analysis and design of road superstructure with empirical methods have been widely applied in current practice. The efforts involving the use of analytical methods and approximate analytical methods have also been made. Although the mechanistic method is more reliable than empirical methods, the effectiveness of any mechanistic design method relies on the accuracy of stress and strain predictions [2]. The biggest obstacle in the transition to the fully analytical design are numerous factors affecting road structures and their design, such as the environment, climate, water content, axle load, number of axle repeats, wheel dimensions, physical and mechanical properties of materials used in road construction, mixing ratios, and grain size diameter.

According to the literature on the analysis of road structures under moving loads, current numerical methods involve the finite element method (FEM), the boundary element method (BEM), or the combination of FEM/BEM methods [3]. The use of numerical methods for the analysis of road structures has greatly increased over the past two/three decades, in parallel with the development of computer technology.

Two-dimensional (2D) or three-dimensional (3D) finite element methods have been increasingly used in recent years in the analysis of flexible pavements because of their flexibility and as they provide the opportunity for changing stress conditions, material sets, water table conditions, and other inputs.

Various computer programs based on elastic layered theory have been developed since the introduction of computers in road design [4]. The earliest and the best-known software of this kind is the CHEV program [5]. The program was later on modified to account for the nonlinear elastic behaviour of granular materials [6]. Other programs such as BISAR, ELSYM5 and KENLAYER have also been developed based on the elastic layered theory [7, 8]. Computer programs ILLI-PAVE and MICH-PAVE have equally been developed for road analysis, but based on stress dependent behaviour of materials and the use of the FEM method [9, 10].

Commercial finite element programs such as ABAQUS, ANSYS, and LS-DYNA, developed for general finite element

analyses, have also been used in road design. These programs provide an opportunity to use more sophisticated material models. Plaxis is also a commercial finite element software that has been developed at the University of Delft, and its use has been extended to the field of geotechnical engineering. Thus, Plaxis is a finite element program that is widely used for 2D and 3D analysis of geotechnical structures, and it enables the use of many material models. In addition, many researchers have used Plaxis software to analyse road pavements and road superstructures reinforced with geotextile so as to decide to which depths geotextile should be placed. This software is also used for analysing road pavements reinforced with piles, and for analyses based on some other methods [11-16].

On the other hand, permanent deformations under traffic loads have a critical role in the long-term performance of roads [17]. Therefore, various permanent deformation models have been developed in literature. A stress-dependent permanent deformation model of an unbound layer of road pavement, developed by Korkiala-Tanttu [18], consists of two parts: the first part shows the load number dependency, and the second part displays the stress dependency, which is represented with the failure ratio. The model is based on laboratory tests, Heavy Vehicle Simulator tests, and stress analysis according to the finite element method. The Plaxis analysis was conducted for the stress dependency factor, while behaviour of materials was represented with both Mohr-Coulomb (MC) and Hardening Soil models (HS). It was established that permanent deformation of unbound granular materials depends on the number of load passes, material strength parameter, failure ratio, water content, and degree of compaction.

In the study conducted by Erlingsson and Saevarsdottir [12], the result of permanent deformation of flexible pavement layers modelled with the HS Model was found compatible with the results obtained according to the Accelerated Pavement Test. For the long term dynamic simulation of road pavement, a more realistic result can be obtained if the soil-asphalt interaction is also taken into account [19].

The main objective of this study is to develop a new long term permanent deformation model of layered flexible road pavements by using the finite element method, which provides an opportunity to account for interaction between layers. Two-dimensional axial symmetric finite element analyses are performed to predict deformation behaviour of road cross-sections. It has been observed that permanent deformation consists of two linear parts when the vertical permanent deformation is plotted versus the log-scaled load number. The slope of the permanent deformation curve increases after a certain load level is exceeded.

## 2. Pavement sections

Conventional flexible pavements consisting of hot mix asphalt layers are supported by the underlying unbound granular base layers. The base layer can consist of one or more layers, such as base and subbase layers. The number of base layers and their thicknesses are dependent on the number of load cycles occurring during the service life of the road, magnitude of load, strength of layers, and weather conditions.

The typical pavement cross-section analysed in this study is given in Figure 1. The cross-section consists of an asphalt concrete (AC) layer, base layer, and subbase layers. This structure lies on the natural subgrade layer.

Steel slag is used in many civil engineering applications. More common worldwide applications of steel slag involve its use in the asphalt aggregate, fill material, cement additive, soil improvement, gabions, railway ballast, road base, riprap, including also its applications in environment and agriculture.

Four pavement cross-sections, given in Figure 2, were analysed by using steel slag in different pavement layers. When used in road base layers, steel slag can be a good alternative to natural aggregate in terms of its mechanical properties. By this way, natural resources can be preserved and some of environmental problems can be avoided. Moreover, establishment of a symbiotic relation between road construction and steel making industry by using steel slag in road construction will result in sustainability of steel making industry, while also resolving steel slag storage problems. Compared to other construction activities, road construction sector is one of the biggest consumers of natural materials. Therefore, steel slag can be one of the main alternatives to the use of natural resources.

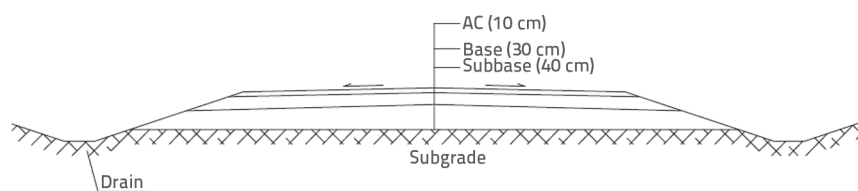


Figure 1. Typical flexible pavement cross-section

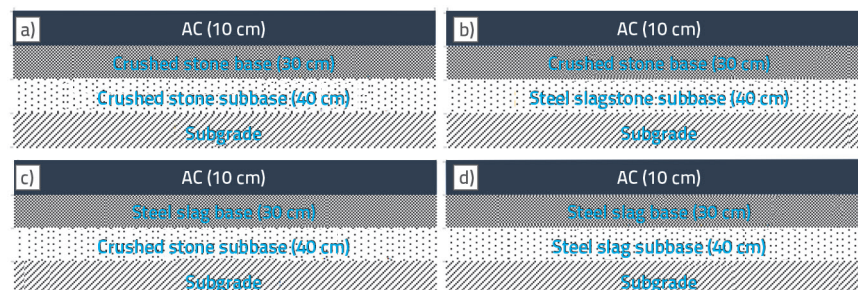


Figure 2. Cross-sections analysed in numerical model: a) CC (crushed stone base, crushed stone subbase); b) CS (crushed stone base, steel slag subbase); c) SC (steel slag base, crushed stone subbase); d) SS (steel slag base, steel slag subbase)

The AC layer used in cross-sections is 10 cm in height and it lies on the granular base layer. Thicknesses of base and subbase layers are 30 cm and 40 cm, respectively. Resonant column tests were carried out to determine the small strain shear modulus of steel slag. The crushed stone included in analyses and shown in Figure 2 is the Florida lime rock. Its shear modulus was determined in previous studies using the resonant column test [20].

A two-dimensional axisymmetric model consisting of fifteen-node triangular elements was used for numerical solution (Figure 3).

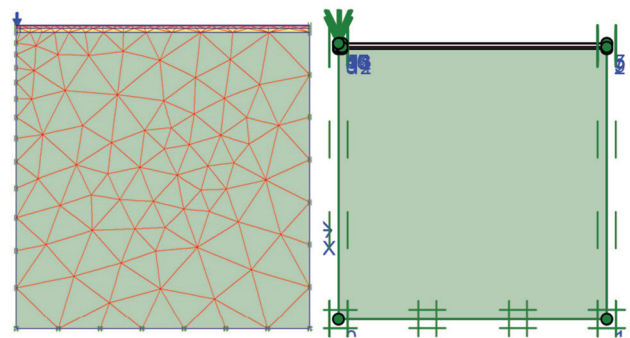


Figure 3. General view of the finite element model

The standard fixity was used for boundary conditions. The model consisted of 307 elements with a total of 2579 nodes. The base of geometry was fixed in each direction and the roller condition was selected for two vertical sides of geometry so that deformation was not restrained in vertical direction because of loading conditions. Finer elements were applied around the wheel load in the base and subbase layers in order to obtain reliable results. On the other hand, to reduce calculation time, coarser elements were used towards the edges of model.

Numerical model measures 30 m in height and 30 m in width. It means that the model size in both directions is selected about 100 times of loading diameter. These are appropriate dimensions for neglecting the effects of boundary conditions, which is in line with recommendations made by previous researchers [21-23].

## 3. Materials and response models

This study, based on the finite element method, focuses on deformation behaviour of flexible road pavements as

a function of load cycles. Soil stiffness changes with the stress and strain rate and it is also sensitive to unloading-reloading conditions. A part of the loading energy is dissipated at each load cycle because of damping. Soil behaves elastically at small strain levels. Plastic deformation occurs after a certain strain level is exceeded. Stiffness of soil decreases with an increase in strain level. Nonlinearity is another characteristic of soil related to stiffness decrease with an increase in strain. According to previous studies, the stiffness decrease function is S-shaped when drawn versus log scaled strain (Figure 4) [24].

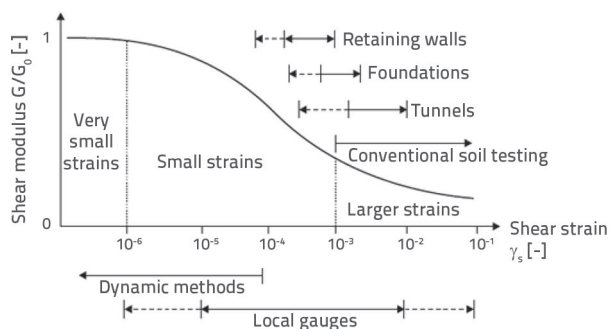


Figure 4. Characteristic stiffness-strain behaviour of soil with typical strain ranges for laboratory tests and structures [24]

Road pavements are under the influence of traffic loads and natural conditions. Traffic loads create radial tension and compressive stresses as well as vertical compressive stresses during vehicle movements. The magnitude and extent of the stresses are directly proportional to the repetition and magnitude of axle loads [25]. The magnitude of strain will increase with an increase in axle load repetition. Unbound materials used in pavement layers are under unloading/reloading conditions because they are subjected to repetitive traffic load. The direction and magnitude of the stress path change during each cycle. The constitutive model of unbound

pavement materials should respond to stress dependency and unloading/reloading conditions, and should also take into account the reduction of stiffness with an increase in strain. Because of having the capability of unloading/reloading, model reduction with an increase in strain, and hysteretic damping, the Hardening Soil Model with Small Strain (HSsmall) was applied as a constitutive model for unbound materials used in road base layers and subgrade layers. Despite some limitations, such as the independent formulation of the void ratio and the lack of kinematic hardening, the adequacy of HSsmall has been demonstrated in a number of geotechnical applications [26].

Since asphalt concrete is composed of aggregates, water and air, it is analogous to soil which is composed by solids, water, and air [27]. So, at intermediate temperatures, asphalt can be modelled as a Mohr-Coulomb material with both cohesive and granular properties [28]. The internal friction angle of asphalt concrete is a function of aggregate and interlocking, whereas cohesive properties of asphalt depend on bitumen properties and temperature [29]. Based on previous studies, the internal friction angle of asphalt concrete is greater than 40°, and its cohesion amounts to approximately 500 kPa at 25°C. In some experimental studies, the internal friction angle of approximately 46° was obtained at the same temperature [27, 28]. In this study, the subgrade and unbound materials used in the road base and subbase were modelled using the HSsmall soil model. The AC layer was modelled with the Mohr-Coulomb material model. The deformation characteristic of steel slag was obtained by performing the resonant column test. According to previous experimental results, the internal friction angle of steel slag is taken to be 47° and 45° for the base layer and the subbase layer, respectively, and its cohesion is taken to be 45-47 kPa [30, 31]. All materials properties used in this study are listed in Table 1.

The HSsmall implemented in the commercial program Plaxis is based on the HS model and uses the same parameters. However, HSsmall has two additional parameters for describing the reduction of stiffness with an increase in strain. These two parameters are the small strain stiffness of soil ( $G_0$ ) and the

Table 1. Material properties used for the study

Properties	Asphalt (AC)	Base (crushed stone)	Subbase (crushed stone)	Subgrade (clay)	Base (steel slag)	Subbase (steel slag)
Thickness [m]	0.1	0.30	0.40	10.0	0.30	0.40
G0ref [MPa]	-	185	128	55	180	138
E50ref [MPa]		165	115	24	160	124
Eref [MPa]	4500					
$\nu$ (Poisson ratio)	0.30	0.35	0.35	0.20	0.35	0.35
Cohesion [kN/m <sup>2</sup> ]	500	40	40	100	47	45
$\phi$ (Friction angle) [°]	46	40	35	10	47	45
Rayleigh damping		5 %	5 %	5 %	5 %	5 %

threshold shear strain ( $\gamma_{0.7}$ ), as shown in the following equations: (1) and (2):

$$G_0 = G_0^{ref} \left( \frac{c \cos f - \sigma_3' \sin f}{c \cos f + p^{ref} \sin f} \right)^m \quad (1)$$

$$\gamma_{0.7} = \frac{1}{9G_0} \left[ 2c'(1 + 2 \cos \phi') + \sigma_1'(1 + k_0) \sin 2\phi' \right] \quad (2)$$

where  $G_0^{ref}$  is the shear modulus at very small strain of  $\varepsilon < 10^{-6}$ , corresponding to the reference pressure ( $P_{ref}$ ) of 100 kPa, and  $m$  is the power for stress-level dependency of stiffness.

In the HSsmall model, the secant shear modulus is formulated in accordance with suggestions given by Santos and Correia [32], as shown in Eq. (3):

$$G_s = \frac{G_0}{1 + 0.385 \frac{\gamma}{\gamma_{0.7}}} \quad (3)$$

where  $\gamma_{0.7}$  is the threshold shear strain at  $0.7G_0$ , as given in Eq. (2).

#### 4. Permanent deformation

One of the main aspects of the design philosophy for flexible pavements is the limitation of ruts in pavement structure. Measuring rut development is relatively simple, but the prediction of rut development is extremely complex. The problem is not only to characterize the pavement materials but also to assess the impact of the environmental conditions and calculate the appropriate stress distribution during the entire service life of the pavement [33].

The rutting under load is a function of load level, number of load cycles, and material parameters. When evaluated in terms of material, permanent deformations are caused by compaction, crushing, and migration of material [34]. Of course, these changes occurring in materials are a function of material type, grain size distribution, density, and moisture content [35].

According to the shake down theory that has been used quite extensively in recent times, the response of unbound granular materials to cyclic loading can be defined in three ranges. These ranges are the plastic shakedown range, plastic creep range, and incremental collapse range. In the plastic shakedown range the material is subjected to a relatively low stress level. In the plastic creep range, the material is under a medium stress level. In this range, the permanent deformation rate per cycle is nearly constant after a certain number of load cycles. The number of load cycles required for reaching this constant level of strain rate is dependent on the material and the load level. This number of load cycles may show the end of post-compaction [36]. In the incremental collapse range, the stress level is higher compared to the plastic shakedown range and the plastic creep range. The failure condition is eventually reached in this range [37, 38].

The vertical permanent strain line can be divided in three phases. In the first phase (post compaction), the permanent deformation is mainly forced by particle reorientation and breakage. It results in volumetric change due to densification. In the second phase, the permanent strain rate per cycle is nearly unchanged and is mostly caused by attrition due to particle contacts rather than by particle breakage. After many second phase cycles, the strain rate begins to increase and results in collapse. In this last phase, the grain attrition contributes to collapse [36].

Barksdale [39] found that the permanent axial deformation rises linearly with the logarithm of load cycles under constant deviator stress. Test results show possible sudden rise increment in permanent deformation after a high number of load cycles.

According to literature, in most permanent deformation models, there is an exponential relation between the load cycle and deformation. The more common and simplest equation proposed in [40] is presented in Eq. (4):

$$\varepsilon_p = aN^b \quad (4)$$

where  $\varepsilon_p$  is the permanent axial strain,  $a$  and  $b$  are regression parameters, while  $N$  is the number of load cycles.

Korkiala-Tanttu [18] developed a new nonlinear elastoplastic model. The deformation model's equation is founded on the theory of static load, which is extended to the cases of dynamic load. This equation is given below:

$$\varepsilon_p = CN^b \frac{R}{1-R} \quad (5)$$

where  $\varepsilon_p$  is the permanent vertical strain,  $R$  is the deviator stress ratio,  $b$  is the shear ratio parameter depending on the material, and  $C$  is the material parameter depending on the compaction and saturation level.

Huurman [41] performed Repeated Load Triaxial tests to determine the permanent deformation behaviour of different sands. Finally, the log-log approach of the stress-dependent permanent deformation model of unbound materials, which consists of two terms, was developed in [41]. In this model, the first term represents the deformation occurring at stable behaviour. The second term was added so as to represent the unstable behaviour phase of the material.

The Dresden model was developed at Dresden Technical University [36] based on the existing model [41]. In the Hurman model [41], the first term represents a linear increase in the permanent strain ( $\varepsilon_p$ )-load cycle ( $N$ ) relation in logarithmic scale.  $A$ ,  $B$ ,  $C$ , and  $D$  are the stress-dependent coefficients of the model and depend on the  $\sigma_1/\sigma_{1f}$  ratio.  $\sigma_1$  and  $\sigma_{1f}$  are the major principal stress, and the major principal stress at failure, respectively. Instead of using the  $\sigma_1/\sigma_{1f}$  ratio, Werkmeister [36] redefined the  $A$  and  $B$  parameters as a function of principal stresses  $\sigma_1$  and  $\sigma_3$ . The Dresden model is presented in the following equation:

$$\epsilon_p = A\left(\frac{N}{1000}\right)^B + C(e^{\frac{D \cdot N}{1000}} - 1) \tag{6}$$

where  $\epsilon_p$  is the permanent vertical strain, N is the number of load cycles. A, B, C, D are stress-dependent model coefficients, while  $\sigma_1$  and  $\sigma_3$  are the major and minor principal stresses, respectively.

As stated in [36], the first term represents the permanent strain of the second phase as defined above for the first two stress ranges of the shakedown theory. A and B have different functions for each deformation phase. The second term represents behaviour at a higher stress level, at the third stress range (incremental collapse range) of the shakedown theory. Because the test data in the study were insufficient for recognizing the collapse, the stress dependent parameters C and D were not defined in the Dresden model.

Instead of determining the total permanent deformations by summing up the calculated permanent deformations obtained in each layer, this study focuses on the total deformation/rutting of the road cross-section by using the FEM analysis for studying the layer interaction behaviour. The relation between the rutting and load number is analysed using the two-dimensional finite element method with axisymmetric analyses.

### 5. Analysis and results

Most research efforts on deformation characteristics of unbound materials used in road pavements have so far been focusing on the deformation of each unbound material considered separately in a particular road layer [18, 36]. As it is well known in geotechnical engineering, layers in multi-layered soil behave differently under dynamic load when compared to individual load imposed on single layers, which is due to interaction between these layers. In a layered system subjected to dynamic loading, some of the energy is reflected in the interface between layers, some of the energy is transmitted, while some is dissipated because soil layers are characterised by different flexibility and density values. Instead of studying deformation characteristics of each layer used in road section, this study focuses on the total deformation/rutting of the surface. Road sections analysed in this study are a multi-layered system consisting of asphalt concrete (AC), base layer, and sub-base layers with different rigidity and density values.

Stress pulses can be assumed as haversine or triangular loading. The duration of load depends on the vehicle speed and the depth of the point below the pavement surface [21, 42]. For representing the haversine load in a programme, at least six sub-steps are needed for each load step. However, only two sub-steps are needed for the triangular load pulse without the rest time. Since a lower storage capacity is needed, and as computational time can be reduced due to lower number of sub-steps [43], the triangular load intensity was preferred in this study to haversine load. The compressive

triangular pulse load with 0.144 second load duration, at a tire pressure of 400 kPa, is used for the analysis (Figure 5). This pressure is a rounded value for a standard single axle load of 80 kN for the squared tire contact area with the 300 mm edge length.

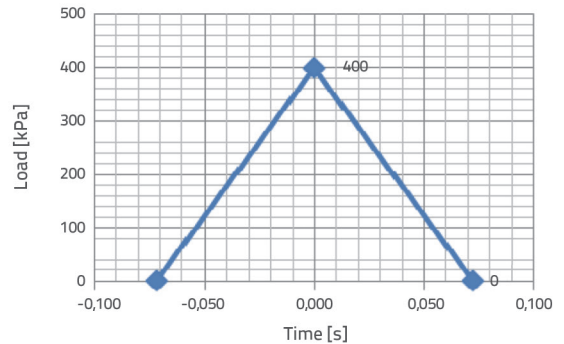


Figure 5. Dynamic stress pulse

After application of 20.111 load cycles, the permanent vertical deformation of pavement surface for centre of load, versus load cycles, is plotted below for four analysed pavement sections as defined in Figure 2. Numerical results for each cross-section are given in Figure 6.

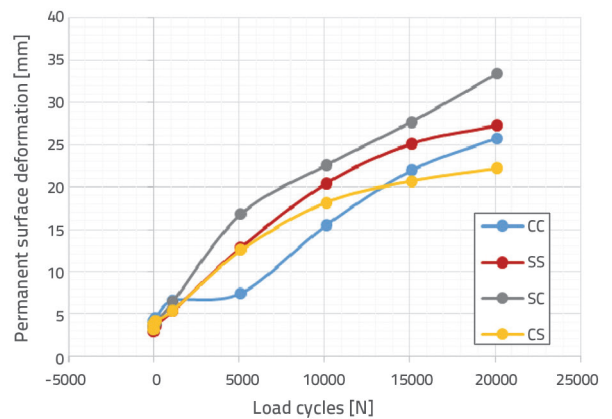


Figure 6. Surface deformation-load cycles

According to Figure 6, the highest deformation was obtained in the cross-section CC for the first 1,000 load cycles. Between 2,000 and 13,000 cycles, the cross-section CC presented the lowest deformation compared to other cross-sections. After 13,000 cycles, the lowest deformation was exhibited by the cross-section CS. These results show that analyses should be carried out with a sufficient number of load steps so as to enable proper estimation of the long-term permanent deformation.

There is a different deformation tendency in the CC deformation curve shown in Figure 6. The stiffness contrast or difference of CC section for granular base and subbase

had the highest value when compared with the remaining three cross-sections. This was probably caused by different deformation tendencies.

When vertical permanent deformation is plotted versus the log-scaled load number, the permanent deformation/log-scale function consists of two linear parts, as shown in figures 7 to 10. In the first part, permanent deformation increases linearly with the load cycle. This indicates that the pavement is in stable condition. The permanent deformation curve slope increases after this threshold load number is exceeded. This permanent deformation behaviour is compatible with Dresden Model [36] and Barksdale [39] study which consists of two parts. But, according to figures 7 to 10, the threshold load number is different for each cross-section under study. Because each cross-section has different void ratio and different strength, the same load condition causes different deformation graphs and different breakpoints. The other reason can be different energy dissipation for each cross-section, as caused by different layering conditions. The permanent deformation graphs of each cross-section versus load cycles, and their permanent deformation functions, are given below.

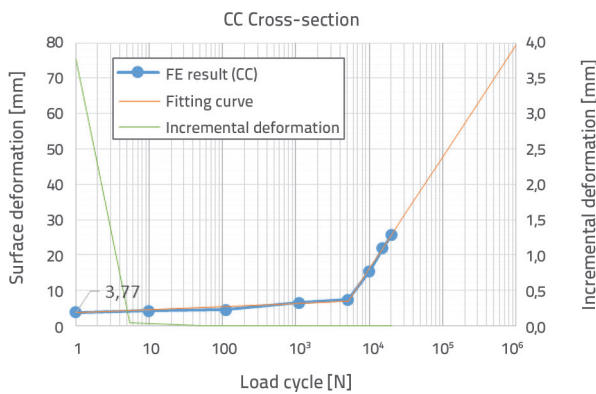


Figure 7. Deformation-load cycles for cross-section CC

$$\begin{aligned}
 sN_1 &= 3.77 \text{ mm} \\
 \Delta S_1 &= sN_1 + C_1 \text{Log}(N/1) \quad N \leq 5100 \quad (C_1 = 0.871) \\
 \Delta S_2 &= sN_{5100} + C_2 \text{Log}(N/5100) \quad N \geq 5100 \quad (C_2 = 31.545)
 \end{aligned}
 \tag{7}$$

where  $sN_1$  is the deformation for the first cycle,  $C_1$  is the slope of the first line when load number is under 5100,  $C_2$  is the slope of the second line when load number is greater than 5100. In the cross-section CC (crushed rock base + crushed rock subbase), the threshold load number is 5100 under the 400 kPa load pulse. After this load number, the permanent deformation slope rises in the semi-log scaled curve (Figure 7).

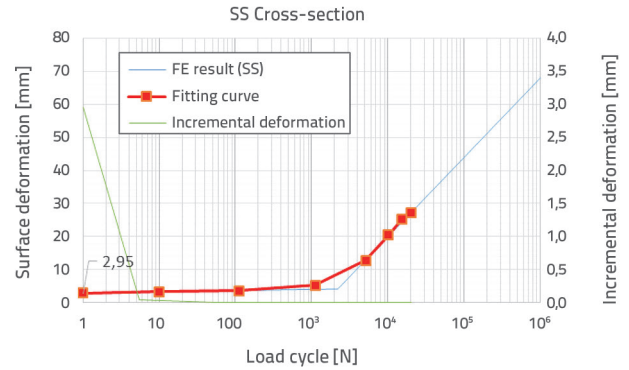


Figure 8. Deformation-load cycles for cross-section SS

$$\begin{aligned}
 sN_1 &= 2.95 \text{ mm} \\
 \Delta S_1 &= sN_1 + C_1 \text{Log}(N/1) \quad N \leq 2200 \quad (C_1 = 0.374) \\
 \Delta S_2 &= sN_{2200} + C_2 \text{Log}(N/2200) \quad N \geq 2200 \quad (C_2 = 24.006)
 \end{aligned}
 \tag{8}$$

where  $sN_1$  is the deformation for the first cycle,  $C_1$  is the slope of the first line when load number is under 2200,  $C_2$  is the slope of the second line when load number is greater than 2200. In the cross-section SS (steel slag base + steel slag subbase), the threshold load number is 2200 under the 400 kPa load pulse. After this load number, the permanent deformation slope rises in the semi-log scaled curve (Figure 8).

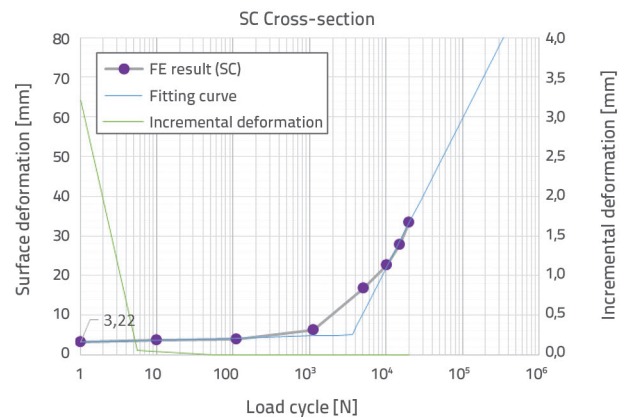


Figure 9. Deformation-load cycles for cross-section SC

$$\begin{aligned}
 sN_1 &= 3.219 \text{ mm} \\
 \Delta S_1 &= sN_1 + C_1 \text{Log}(N/1) \quad N \leq 3600 \quad (C_1 = 0.529) \\
 \Delta S_2 &= sN_{3600} + C_2 \text{Log}(N/3600) \quad N \geq 3600 \quad (C_2 = 37.913)
 \end{aligned}
 \tag{9}$$

where  $sN_1$  is the deformation for the first cycle,  $C_1$  is the slope of the first line when the load number is under 3600,  $C_2$  is the slope of the second line when the load number is greater than 3600. In the cross-section SC (steel slag base + crushed rock

subbase), the threshold load number is 3600 under the 400 kPa load pulse. After this load number, the permanent deformation slope rises in the semi-log scaled curve (Figure 9).

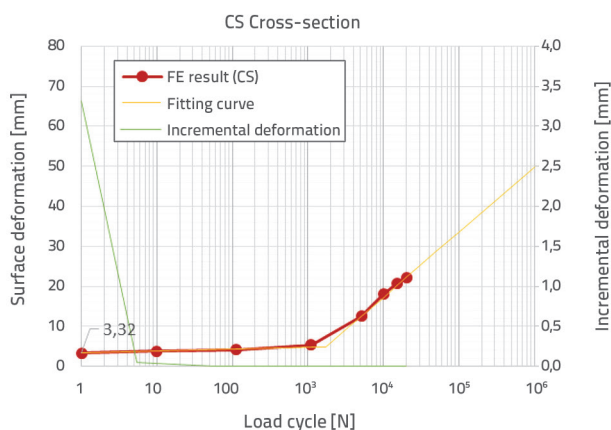


Figure 10. Deformation-load cycles for cross-section CS

$$\begin{aligned}
 sN_1 &= 3.320 \text{ mm} \\
 \Delta S_1 &= sN_1 + C_1 \text{Log}(N/1) \quad N \leq 1700 \quad (C_1 = 0.458) \\
 \Delta S_2 &= sN_{1700} + C_2 \text{Log}(N/1700) \quad N \geq 1700 \quad (C_2 = 16.248) \quad (10)
 \end{aligned}$$

where  $sN_1$  is the deformation for the first cycle,  $C_1$  is the slope of the first line when the load number is under 1700,  $C_2$  is the slope of the second line when the load number is greater than 1700. In the cross-section CS (crushed rock base + steel slag subbase), the threshold load number is 1700 under the 400 kPa load pulse. After this load number, the permanent deformation slope rises in the semi-log scaled curve (Figure 10).

The average stiffness of unbound layers and their average void ratio for each cross-section, and the information about four graphs, is summarized in table below.

Permanent deformation curves consist of two different parts with different slopes. In all deformation graphs, it is pointed out that different deformation phases are obtained as stated by previous studies. The first part represents the post compaction phase. In this phase, deformations are due to reorientation of particles and these deformations result in volumetric change. The second phase deformations are

mostly caused by attrition at the contact between particles. It can be seen in Table 2 that the slope change point is different in each curve, and that the curves also differ according to their short- and long-term deformation parameters.

According to four analysis results summarized in Table 2, it can be seen that there is an inverse relation between the slopes of the second part of each graph ( $C_2$ ) and the average rigidity of unbound layers. The inverse relation between the average rigidity of unbound layers and the long-term deformation can also be noted because  $C_2$  has a major effect on long term deformation. The long-term deformation is forced by the total rigidity of unbound granular materials according to Table 2. The higher the average stiffness of unbound materials, the lower the deformation under high load cycles. However, there is no meaningful relation between the total rigidity of unbound layer and the short-term deformation parameters  $C_1$ ,  $sN_1$  and  $\Delta S_1$ .

When the same material is selected for the base layer or subbase layer, the meaningful relation is obtained between the rigidity difference and the short-term deformation parameters  $C_1$  and  $\Delta S_1$ .  $C_1$  and  $sN_1$  represent the first line slope and the initial deformation for the first load cycle, respectively.  $\Delta S_1$  is the deformation at the threshold load number at which the slope of the curve changes. The higher the rigidity difference of unbound layers is selected, the higher short-term parameters like  $C_1$  and  $\Delta S_1$  are obtained. In addition, no correlation was established between stiffness parameters and the threshold load number.

Different threshold obtained with the load cycle number for each cross-section, and the effect of stiffness contrast on some outputs, point to the layer interaction behaviour of road cross-sections under repetitive traffic loads.

## 6. Conclusion

The deformation behaviour of flexible road pavements as a function of load cycles is analysed in this study using the finite element method. The HSmall model is used for representing unbound granular materials and the subgrade layer. Maximum shear deformation modulus ( $G_{max}$ ) of unbound materials is determined using the resonant column test.

A new vertical permanent deformation approach is used in

Table 2. Summarized information from deformation graphs

Cross-Section	Rigidity Base/Subbase [MPa]	Rigidity difference [MPa]	Average rigidity of unbound layers [MPa]	Average void ratio of unbound layers (e)	$N_{threshold}$	$C_1$	$C_2$	$sN_1$ [mm]	$\Delta S_1$ [mm]	$\Delta S_2$ [mm]
CC	185/128	57	152	0.586	5100	0.871	31.545	3.77	7.00	25.80
SS	180/138	42	156	0.596	2200	0.374	24.060	2.95	4.20	27.30
SC	180/128	52	150	0.590	3600	0.529	37.913	3.22	5.10	33.40
CS	185/138	47	158	0.591	1700	0.458	16.248	3.32	4.80	22.20



this study. Instead of determining deformation characteristics of each layer used in the road section, this study focuses on the total deformation/rutting of the surface. Road sections analysed in this study are a multi-layered system consisting of asphalt concrete (AC), base layer, and sub-base layers, with different rigidity and density values.

When vertical permanent deformation is plotted versus the log scaled load number, it can be observed that the permanent deformation-log scale function consists of two linear parts. In the first stage, at some load cycles, the permanent deformation increases linearly with the load cycle. It can be stated that the pavement is in stable condition in the first stage of the deformation graph. The slope of the permanent deformation curve increases after the mentioned load cycles are exceeded. This permanent deformation behaviour is compatible with Dresden Model. However, there is no constant break point in deformation graphs. The turning point of the semi log scaled deformation graph varies for each cross-section, and the slopes of the first and second lines also vary for each graph.

Two different unbound materials are used as unbound granular materials. Different threshold load number is obtained for each cross-section under study. The results show that vertical deformation graphs have the same

tendency but with different slopes, and also with a different threshold load number.

The second line slope ( $C_2$ ) is inversely correlated with an average unbound layer stiffness. Besides, the slope of the first line ( $C_1$ ) is also inversely correlated with the strength difference of unbound layers. In addition, there is no correlation between the strength or stiffness parameter and  $sN_1$ .

As a result, a road structure is a combined layered system consisting of the subgrade, unbound granular layers, and an asphalt layer. Besides evaluating deformation characteristics of each layer used in the road cross-section by means of laboratory studies, the total deformation of road cross-sections should also be checked using numerical methods in order to determine the layer interaction behaviour. To determine the long-term behaviour of flexible roads under traffic load using numerical analyses, a sufficient number of load steps should be selected for obtaining the second part of the deformation graph. The numerical analysis should be carried out for each distinct cross-section and for different subgrade conditions in the road line. Only some of the parameters effecting road structures are analysed in this study. Different load levels, changes in climate conditions and water table, a higher stiffness contrast, and other variables, should equally be considered in further studies.

## REFERENCES

- [1] Hai-lin, Y., Wan-ping, W., Ping, C.: Dynamic stress and deformation of a layered road structure under vehicle traffic loads: Experimental measurements and numerical calculations, *Soil Dynamics and Earthquake Engineering*, (2012) 39, pp. 100–112
- [2] Wang, J.: Three-Dimensional Finite Element Analysis Of Flexible Pavements, The University of Maine, MSc., Main, 1996.
- [3] Beskou, N.D., Theodorakopoulos, D.D.: Dynamic effects of moving loads on road pavements: A review, *Soil Dynamics and Earthquake Engineering*, 31 (2011) 4, pp. 547–567
- [4] Burmister, D.M.: The general theory of stresses and displacements in layered soil systems, *Journal of applied Physics*, 16 (1945) 5, pp. 296–302
- [5] Warren, H., Dieckmann, W.: Numerical computation of stresses and strains in a multiple-layer asphalt pavement system, International Report, Chevron Research Corporation, Richmond, CA, 1963.
- [6] Hwang, D., Witczak, M.: Program DAMA (Chevron), User's Manual, Department of Civil Engineering, University of Maryland, 1979.
- [7] De Jong, D., Peutz, M., Korswagen, A.: Computer program BISAR - Layered systems under normal and tangential surface load, External Report No. AMSR.006., Amsterdam, 1979.
- [8] Kopperman, S., Tiller, G., Tseng, M.: Elsym5 Interactive microcomputer version, User's Manual, Report No. FHWA-TS-87-206, Federal Highway Administration, 1986.
- [9] Harichandran, R., Baladi, G., Yeh, M.: Development of a computer program for design of pavement systems consisting of bound and unbound materials, Department of Civil and Environmental Engineering, Michigan State University, 1989.
- [10] Qiu, Y., Dennis, N.D., Elliott, R.P.: Stress distribution in subgrade soils and applications in the design of flexible pavements, 30 (1999), pp. 221–233
- [11] Firat, S.: Stability analysis of pile-slope system, *Scientific Research and Essays*, 9 (2009) 4, pp. 842–852
- [12] Saevarsdottir, T., Erlingsson, S.: Deformation Modelling of Instrumented Flexible Pavement Structure, *Procedia engineering*, 143 (2016), pp. 937–944
- [13] Al-Jumaili, M.: Finite element modelling of asphalt concrete pavement reinforced with geogrid by using 3-D plaxis software, *International Journal of Materials Chemistry and Physics*, 2 (2016) 2, pp. 62–70
- [14] Hashem, M.D., Abu-Baker, A.M., Hashem, M.D.: Numerical Modeling of Flexible Pavement Constructed On Expansive Soils, *Eur. Int. J. Sci. Tech*, 10 (2013) 2, pp. 19–34
- [15] Kazemian, S., et al.: Reinforced pavement above trench under urban traffic load: Case study and finite element (FE) analysis, *Scientific Research and Essays*, 21 (2010) 5, pp. 3313–3329
- [16] Ouf, M.S., et al.: Evaluation of Stabilized Pavement Sections Using Finite Element Modeling, *International Journal of Scientific & Engineering Research*, 7 (2016) 4, pp. 1749–1756

- [17] Rahman, M.S.: Characterising the Deformation Behaviour of Unbound Granular Materials in Pavement Structures, Division of Highway and Railway Engineering, Department of Civil and Architectural Engineering, KTH Royal Institute of Technology, PhD, 2015.
- [18] Korkiala-Tanttu, L.: Calculation method for permanent deformation of unbound pavement materials, Department of Civil and Environmental Engineering, Helsinki University of Technology, 2008.
- [19] Ghadimi, B., Nega, A., Nikraz, H.: Simulation of shakedown behavior in pavement's granular layer, *International Journal of Engineering and Technology (IJET)*, 7 (2015) 4, pp. 198-203
- [20] Hiltunen, D.R., Roque, R., Ayithi, A.: Base Course Resilient Modulus for the Mechanistic-Empirical Pavement Design Guide, University of Florida, Department of Civil and Coastal Engineering, Florida, 2011.
- [21] Huang, Y.H.: *Pavement Analysis and Design*, 2th ed., Pearson Prentice Hall, NJ, 2004.
- [22] Duncan, J.M., Monismith, C.L., Wilson, E.L.: Finite element analysis of pavements, *Highway Research Record*, 228 (1968), pp. 18-33
- [23] Kim, M.: Three-dimensional finite element analysis of flexible pavements considering nonlinear pavement foundation behavior, University of Illinois Urbana, Illinois, 2007.
- [24] Atkinson, J.H., et al.: Experimental determination of soil properties, *Proceedings of 10th ECSMFE*, Florence, 1991.
- [25] Güngör, A.G., Sağlık, A.: *Karayolları Esnek Üstyapılar Projelendirme Rehberi*, T.A.D.B.Ü.Ş. Müdürlüğü, KGM, Ankara, 2008.
- [26] Benz, T.: Small-strain stiffness of soils and its numerical consequences, Univ. of Stuttgart, Inst. of Geotechnik, PhD, Stuttgart, 2007.
- [27] Wang, H., Al-Qadi, I.L.: Near-surface pavement failure under multiaxial stress state in thick asphalt pavement, *Transportation Research Record*, 2154 (2010) 1, pp. 91-99
- [28] Mattos, J., R., Nunez, W., P., Ceratti, J., A., Zingano, A., Fedrigo, W.: Shear strength of hot-mix asphalt and its relation to near-surface pavement failure – A case study in Southern Brazil, *Proceedings of 6th Eurasphalt & Eurobitume Congress*, Prague, 2016.
- [29] Tan, S., Low, B., Fwa, T.: Behavior of asphalt concrete mixtures in triaxial compression, *Journal of Testing and Evaluation*, 22 (1994) 3, pp. 195-203
- [30] Nouredin, A.S., McDaniel, R.S.: Evaluation of surface mixtures of steel slag and asphalt, *Transportation Research Record*, 1990., pp. 133-149
- [31] Yildirim, I.Z., Prezzi, M.: Use of steel slag in subgrade applications, Final Report, INDOT Office of Research and Development, FHWA/IN/JTRP-2009/32-SPR-3129, Indiana, 2009.
- [32] Dos Santos, J., Correia, A.: Reference threshold shear strain of soil and its application to obtain a unique strain-dependent shear modulus curve for soil, *15th Int. Conf. SMGE*, Istanbul, 1 (2001), pp. 267-270
- [33] Lekarp, F., Isacsson, U., Dawson, A.: State of the art. II: Permanent strain response of unbound aggregates, *Journal of transportation engineering*, 126 (2000) 1, p. 76-83
- [34] Tholen, O.: Falling weight deflectometer, a device for bearing capacity measurements: properties and performance, Degree project, Department of Highway Engineering, Royal Institute of Technology (KTH), Stockholm, 1980.
- [35] Lekarp, F.: Resilient and permanent deformation behavior of unbound aggregates under repeated loading, Royal Institute of Technology (KTH), PhD, Stockholm, 1999.
- [36] Werkmeister, S.: Permanent deformation behaviour of unbound granular materials in pavement constructions, Dresden University of Technology PhD, Dresden, 2003.
- [37] Dawson, A.R., Wellner, F.: *Plastic Behaviour of Granular Materials*, Final Report, ARC Project 933, Reference PRG99014, The University of Nottingham, Nottingham, 1999.
- [38] Werkmeister, S., Dawson, A.R., Wellner, F.: Permanent deformation behavior of granular materials and the shakedown concept, *Transportation Research Record*, 1757 (2001) 1, pp. 75-81
- [39] Barksdale, R.D.: Laboratory Evaluation of Rutting in Base Course Materials, *Proceedings of 3rd International Conference on the Structural Design of Asphalt Pavements*, London, 1972., pp. 161-174
- [40] Sweere, G.T.H.: *Unbound granular bases for roads*, PhD, University of Delft, Delft, 1990.
- [41] Huurman, M.: Permanent deformation in concrete block pavements, Delft University of Technology: Delft, Netherlands, 1997.
- [42] Barksdale, R.D.: Compressive stress pulse times in flexible pavements for use in dynamic testing, *Highway research record*, 345 (1971) 4, p. 32-44
- [43] Karatag, H., Firat, S., Işık, N.S.: Assessment of Performance of Steel Slag Used in Road Base by Finite Element Analysis, *Proceedings of 13<sup>th</sup> International Congress on Advances in Civil Engineering*, Çeşme, İZMİR, 2018.